*Chemistry*

*Physical & Theoretical Chemistry fields*

Okayama University *Year* 1985

# On a homogeneous electrochemical reaction of prussian blue/everitt's salt system

Tsutomu Ohzuku
Okayama University

Keijiro Sawai
Okayama University

Taketsugu Hirai
Osaka City University

# On a Homogeneous Electrochemical Reaction of Prussian Blue/Everitt's Salt System

## A Model of $MnO_2$/MnOOH System

**Tsutomu Ohzuku* and Keijiro Sawai**

*Electrochemistry and Inorganic Chemistry Laboratory, Department of Synthetic Chemistry, Faculty of Engineering, Okayama University, Okayama 700, Japan*

**Taketsugu Hirai***

*Industrial Inorganic Chemistry Laboratory, Department of Applied Chemistry, Faculty of Engineering, Osaka City University, Sugimoto 3-3-138, Sumiyoshi, Osaka 558, Japan*

ABSTRACT

Voltammetric, chronopotentiometric, and spectroelectrochemical studies on the homogeneous-phase (single phase) reaction of Prussian blue (PB)/Everitt's salt (ES) system in KCl aqueous solution were carried out as a model for understanding the homogeneous electrochemical reaction of manganese dioxide. Analytical results of voltammetric and chronopotentiometric studies on PB/ES system indicated that the electrode potential was represented by the empirical formula

$$E = E_0 - (RT/n\mathbf{F}) \ln ([Fe^{2+}]/[Fe^{3+}]) + (RT/\mathbf{F}) \ln [K^+]$$

where the observed $n$ value was 0.5, not 1.0. Results on spectroelectrochemical studies supported the above formulation, and the $n$ value, 0.5, indicated that the effect was thermodynamic, not kinetic. A possible explanation of the problem was given, emphasizing the role of charge carrier in a solid matrix in an electrochemical reaction, and the specific differences between a redox reaction of soluble species in a solution and a redox reaction in a solid matrix were discussed. The electrochemical behavior of $MnO_2$/MnOOH system was deduced in terms of a homogeneous (single phase) electrochemical reaction from the analogy of PB/ES system.

Mixed valence compounds containing an element in two different oxidation states in a crystal lattice offer a class of electrode system unique in electrochemistry. One of the most useful mixed valence compounds is manganese dioxide ($MnO_2$), which is used as a cathode for primary batteries. Reaction mechanism of $MnO_2$ together with the formulation of electrode potential to explain an S-shaped discharge curve has been investigated.

In the discharge process of $MnO_2$, electrons and protons are introduced into the crystal lattice of $MnO_2$ without destroying its essential crystal structure, such as ramsdellite/groutite or pyrolusite/manganite. In other words, the original $MnO_2$ is continuously converted to MnOOH, isostructural with the original $MnO_2$, by increasing $Mn^{3+}$ and $H^+$ (more precisely, $OH^-$) concentration in a crystal lattice during the discharge process. Such an electrochemical reaction may be represented as

$$MnO_2 + H^+ + e^- \rightleftarrows MnOOH \qquad [1]$$

Johnson and Vosburgh (1) and Newmann and Roda (2) gave the reversible reaction [1], and they formulated the electrode potential directly

$$E = E_0 - \frac{RT}{\mathbf{F}} \ln \frac{[MnOOH]}{[MnO_2]} + \frac{RT}{\mathbf{F}} \ln [H^+] \qquad [2]$$

On the other hand, Kozawa and Powers (3, 4) proposed the equation

$$E = E' - \frac{RT}{\mathbf{F}} \ln \frac{[Mn^{3+}]_{solid}}{[Mn^{4+}]_{solid}} \qquad [3]$$

instead of Eq. [2] from the analogy of a redox system in an aqueous solution, emphasizing the homogeneous-phase reaction. They explained the characteristic S-shaped discharge curve of $MnO_2$ fairly well on the basis of homogeneous phase theory (3, 4). Observed S shapes, however, are almost always steeper than those calculated from Eq. [3]. Tye (5) observed −118 mV potential dependence in terms of $\log([Mn^{3+}]/[Mn^{4+}])$ in his electrode potential measurements for composition near to $MnO_2$. The potential dependence, −118 mV, was also observed in open-circuit voltage curves, low rate discharge curves, and potential-decay curves at constant current in alkaline solution for both electrolyte $MnO_2$s and chemically prepared $MnO_2$s (6).

The value, −118 mV, was two times greater than the expected value −59 mV from Eq. [3], which was not observed for a redox reaction in a solution and consequently which may be an essential character of $MnO_2$/MnOOH homogeneous-phase reaction if the effect was thermodynamic. Although there have been several arguments on the electrochemical behavior of $MnO_2$/MnOOH system (7-13), there seems to be general agreement that the electrochemical reduction of $MnO_2$ proceeds in a homogeneous phase and that the behavior resembles that for a redox couple in a solution phase.

There are, however, some differences between a redox reaction in a solution phase and that in a solid phase, *i.e.*, (*i*), the redox couple moving freely in a solution *vs.* the redox couple fixed in a solid matrix, (*ii*) the charge balance due to the movement of ions in a solution *vs.* the movement of foreign ions through a solid matrix, and (*iii*) the specific oxidation state of single ion in a solution *vs.* the nonstoichiometrically average oxidation state due to the formation of polynuclear species in a solid matrix.

Specific differences between a redox reaction in a solution and that in a solid matrix must, therefore, be recognized as to how such differences reflect on the electrochemical behavior of the redox reaction. In order to understand such specific differences between them, the electrochemical and spectroelectrochemical studies on Prussian blue(PB)/Everitt's salt (ES) electrode, the $Fe^{3+}/Fe^{2+}$ redox reaction in a solid matrix, were undertaken.

Physical properties of PB (14-16), such as electronic structure, crystal structure, electronic spectra, molecular magnetism, and the relationship between them are well understood, and reliable methods of preparing thin films of PB chemically (17, 18) and/or electrochemically (19, 20) have been established. Moreover, it is well known that PB having $Fe^{2+}$, $Fe^{3+}$ and bridging CN between them in a cubic lattice is chemically or electrochemically oxidized to Berlin green (BG) isostructural with PB, and also reduced to ES, again isostructural with PB, in an appropriate aqueous solution, indicating that the reaction proceeds in a homogeneous (single) phase. These factors enable us to

*Electrochemical Society Active Member.

study the $Fe^{3+}/Fe^{2+}$ redox reaction in a PB matrix as a model for $Mn^{4+}/Mn^{3+}$ redox reaction in a $MnO_2$ matrix in terms of the solid-state redox reaction.

The objectives of the paper are to give specific differences between a redox reaction in a solution and that in a solid matrix and to give some insights into the electrochemistry of $MnO_2$/MnOOH system out of the experimental and analytical results obtained from PB/ES system.

## Experimental

Thin films of PB were electrochemically prepared on Pt and $In_2O_3$-coated glass electrodes. Electrodes were cathodically polarized at 40 $\mu$A-cm$^{-2}$ for 120s in freshly prepared mixed electrolyte [0.02*M* $FeCl_3$, 0.02*M* $K_3Fe(CN)_6$] at room temperature as was proposed by Itaya *et al.* (19). Thin films of PB deposited on electrodes were rinsed with distilled water to remove undesirable chemical species from the electrode surface. The prepared electrodes were soaked in the same concentrations of KCl solutions as those to be examined for about 3h before use. The prepared sample was identified as PB having a cubic lattice with $a_0$ = 10.2Å by x-ray examination on thick PB on Pt using an x-ray diffractometer (Shimadzu Corporation, Japan, Type XD-3A).

The electrochemical cell consisted of a working electrode, a Pt counterelectrode, and a saturated calomel electrode (SCE) through a Luggin capillary. The electrolytes were solutions having several KCl concentrations and several pH's. The cell was purged with nitrogen gas to remove oxygen from the system.

Cyclic voltammetry was performed using a potentiostat (Kowa Electronics Works Company Limited, Japan, Model PGS-1525) combined with a function generator (Kowa Electronics Works Company Limited, Model FG-101) and the data were recorded on a Houston Model 100 X-Y recorder.

Chronopotentiometry was performed using a galvanostat (Hokuto Denko Company Limited, Japan, Model HA-211). In the case of chronopotentiometry, the thin film of PB on Pt electrode was kept at +0.8 *vs.* SCE until the residual current reduced to less than 1 $\mu$A, and then the control mode was switched over to galvanostat mode. The electrode potential as a function of time was registered on a recorder (Nippon Denshi Kagaku Company Limited, Model U-228).

Optical absorption spectra as a function of electrode potential were measured using a UV-visible spectrophotometer (Shimadzu Corporation, Model UV-240) equipped with a graphic printer (Shimadzu Corporation, Model PR-1). All experimental work was carried out at room temperature.

## Method of Analysis

PB contains $Fe^{3+}$ and $Fe^{2+}$ in different ligand fields in a solid matrix, as is shown in Fig. 1 (21, 22). One is carbon-coordinated iron (low spin), and the other is nitrogen-coordinated iron (high spin). Mössbauer spectra (23, 24) and the magnetic moment (25) of PB suggest the presence of high spin $Fe^{3+}$, and the infrared spectra (26) of CN stretch frequency in PB agree with the ferric ferrocyanide formulation. Mössbauer spectra, however, cannot be positively identified as either $Fe^{2+}$ or $Fe^{3+}$ due to the anomalous isomer shift of iron cyanide (23), and the magnetic data do not determine the structure because they can be explained equally well by high spin $Fe^{2+}$ and low spin $Fe^{3+}$ (14). Thus, there still remains the question which of the two structures, $Fe^{3+}$-NC-$Fe^{2+}$ or $Fe^{2+}$-NC-$Fe^{3+}$, is right (27).

Whichever structure one takes for PB, $Fe^{3+}$ is reduced to $Fe^{2+}$ with no change in the surrounding ligand field. Therefore, we assume that the electrode potential of PB/ES system is determined by the logarithm of the ratio of two oxidation states existing in the same ligand field. Such an electrochemical reaction may be formulated using a general expression by

$$\underset{\text{(solid)}}{\text{Ox}} + ne^- \rightleftarrows \underset{\text{(solid)}}{\text{Red}} \qquad [4]$$

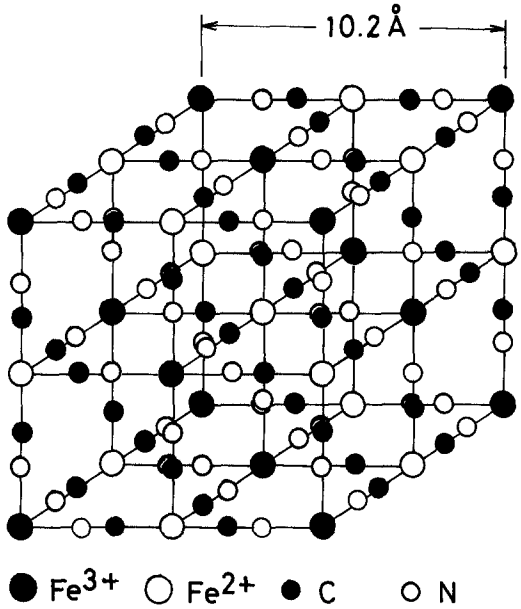


**Fig. 1. Idealized skeleton structure of Prussian blue. In Everitt's salt, $Fe^{3+}$ sites are reduced to be $Fe^{2+}$.**

By applying the Nernst equation directly Eq. [4], the electrode potential is represented as

$$E = E'_0 - \frac{RT}{n\mathbf{F}} \ln\left(\frac{C_R}{C_0}\right) \qquad [5]$$

The condition of an electrochemical reaction in a layered matrix would be formulated as

$$C_0 + C_R = C_T \qquad [6]$$

where $C_0$ and $C_R$ are the surface concentration of Ox and Red, respectively, in moles per square centimeter, and $n$ is the number of electron participating in the electrochemical reaction [4]. $C_T$ is the total surface concentration of species Ox and Red in moles per square centimeter. In fact, $C_0$ and $C_R$ correspond to the surface concentrations of $Fe^{3+}$ and $Fe^{2+}$, respectively, existing in the same ligand field in a solid matrix.

*Voltammetry.*–By solving Eq. [5] with respect to $C_R$ and putting the condition [6] into it, one may have a following expression on the $j$-$E$ characteristics in voltammetry

$$j = -n\mathbf{F}\left(\frac{dC_R}{dt}\right) = Q\frac{\left(\frac{n\mathbf{F}}{RT}\right)\exp\{-\frac{n\mathbf{F}}{RT}(E - E'_0)\}}{|1 + \exp\{-\frac{n\mathbf{F}}{RT}(E - E'_0)\}|^2}\left(\frac{dE}{dt}\right) \qquad [7]$$

where $Q = n\mathbf{F}C_T$, *i.e.*, total charge. Equation [7] was first derived by Hubbard and Anson (28) for a redox reaction in a thin-layered liquid film.

*Chronopotentiometry.*—Assuming Eq. [4]-[6] and setting the additional conditions for chronopotentiometry

$$C_R = 0,\ C_0 = C_T \text{ at } t = 0$$

$$C_R = C_T,\ C_0 = 0 \text{ at } t = \tau$$

and

$$j_C = n\mathbf{F}\left(\frac{dC_0}{dt}\right) = -n\mathbf{F}\left(\frac{dC_R}{dt}\right) \qquad [8]$$

one may have the following expression by solving Eq. [5] under the conditions [6] and [8]

$$E = E'_0 - \frac{RT}{n\mathbf{F}} \ln\left\{\frac{(t/\tau)}{1 - (t/\tau)}\right\} \qquad [9]$$

where $\tau$ is the transition time and $j_C$ is the controlled current.

*Spectroelectrochemical character.*—The broad optical absorption band at ca. 700 nm is characteristic of PB (18, 19). Then, if one assumes that absorbance at *ca.* 700 nm is directly proportional to the concentration of $Fe^{3+}$ existing in a certain ligand field in a PB matrix, as would be expected by Beer's law, one may define the mole fraction of $Fe^{2+}$, $X(E)$, as a function of electrode potential (18) as

$$X(E) = \frac{A_{max} - A(E)}{A_{max} - A_{min.}} \quad [10]$$

and the mole fraction of $Fe^{3+}$, $1 - X(E)$, as

$$1 - X(E) = \frac{A(E) - A_{min.}}{A_{max} - A_{min.}} \quad [11]$$

where $A_{max}$ is a maximum absorbance and $A_{min.}$ is a minimum absorbance when absorbance at *ca.* 700 nm is measured as a function of electrode potential.

Combination of Eq. [5], [10], and [11] gives

$$E = E'_0 - \frac{RT}{n\mathbf{F}} \ln\left(\frac{X}{1 - X}\right) \quad [12]$$

By using Eq. [7], [9], and/or [12], one can determine $E'_0$ and $n$ in Eq. [4] from voltammetric, chronopotentiometric, and/or spectroelectrochemical data.

## Experimental Results

*Voltammetry.*—Figure 2 shows the cyclic voltammograms of PB film on Pt electrode at several sweep rates in 1*M* KCl solution. In recording voltammograms, the initial few cycles were discarded (because the electrode was not well broken in the electrolyte), and then the almost-steady current-potential curves were recorded. The preparation method and pretreatment of electrodes adopted here always gave the same results within an experimental error, and the general observations on voltammograms for PB reduction and ES oxidation agreed well with those of previous workers (17-20).

The voltammetric reduction peaks of PB and oxidation peaks of ES at 200 mV *vs.* SCE were almost symmetrical up to the sweep rate of 100 mV-s$^{-1}$ and had broad half-width of *ca.* 180 mV. The coulombs in and out were almost the same for the reduction of PB and the oxidation of ES. Peak currents increased linearly as a function of sweep rate, not the square root of the sweep rate between 5 and 100 mV-s$^{-1}$, indicating that there were no diffusion problems.

The peak potentials and the midpoints of them were shifted toward anodic direction with increasing KCl concentrations, as a function of $(RT/\mathbf{F})\ln[a_{K^+}]$, suggesting a potential response of potassium ion. No shift, however, was observed in varying solution pH of 1*M* KCl.

Figure 3 shows the comparison between an observed voltammetric curve and the calculated curves from Eq. [7] with $n = 1$ and $Q = 2.5$ mC-cm$^{-2}$. The observed voltammetric curve was much broader than the calculated curve. Equation [7] requires the half-width of 90 mV for $n = 1$, 45 mV for $n = 2$, 30 mV for $n = 3$ and so forth. On the other hand, observed half-widths were about twice the 90 mV which was expected value from Eq. [7] with $n = 1$, and so the $n$ value in Eq. [7] was calculated to be about 0.5.

*Chronopotentiometry.*—In measuring chronopotentiograms for PB reduction, PB on Pt electrode was kept at +0.8V *vs.* SCE until the residual current reduced below a microampere, in order to set the same initial conditions of residual $C_R$ concentrations, and then the control mode was switched over to galvanostatic mode. Transition time $\tau$ was determined as the duration time of potential drop from +0.5 to −0.2V *vs.* SCE. Figure 4 shows the $|j| \cdot \tau$ *vs.* $|j|$ plots for PB reduction in 1*M* KCl solution. The $|j| \cdot \tau$ is almost independent of $|j|$, indicating that the electrochemical reaction took place throughout the PB matrix.

Figure 5 shows a comparison between an observed chronopotentiogram for a PB reduction at 50 $\mu$A-cm$^{-2}$ ($\tau$ = 169s) and the calculated curves from Eq. [9] with $n = 0.5$ and $E'_0 = +0.175$V *vs.* SCE. Although the calculated value of $E'_0$ from chronopotentiogram was *ca.* 25 mV more negative than that from voltammogram, the observed chronopotentiogram, as far as the $n$ value was concerned, agreed well with voltammograms in Fig. 2 and 3.

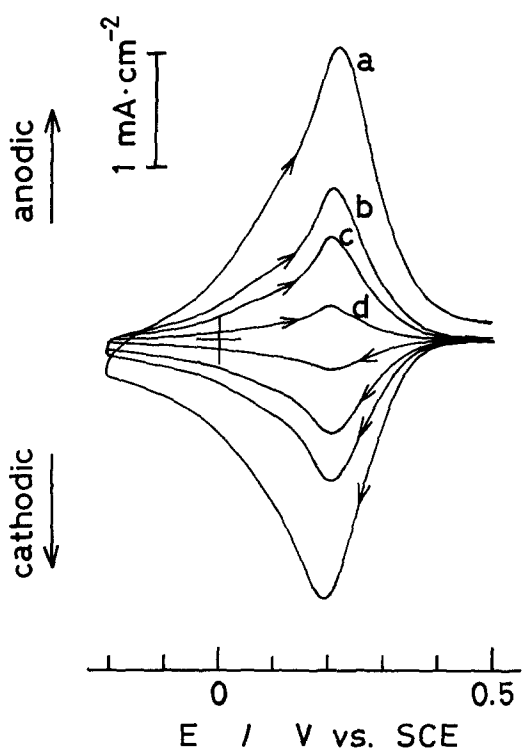


Fig. 2. Voltammograms of a thin film of PB on Pt electrode in 1M KCl solution at room temperature. Sweep rates are 100 (a), 50 (b), 30 (c), and 10 mV-s$^{-1}$ (d).

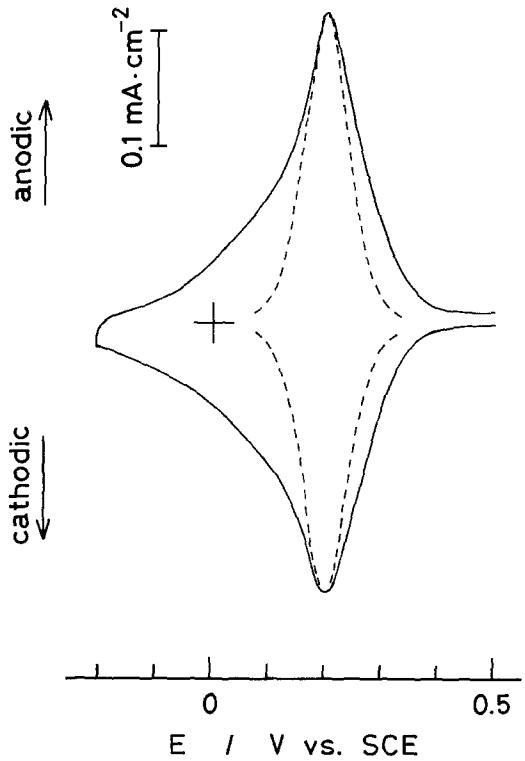


Fig. 3. Comparison between an observed voltammogram for a thin film of PB on Pt in KCl solution at a sweep rate of 10 mV-s$^{-1}$ (solid curve) and the calculated voltammogram from Eq. [7] with $n = 1$, $Q = 2.5 \times 10^{-3}$ C-cm$^{-2}$, and $(dE/dt) = 0.01$ V-s$^{-1}$ (dotted curve).

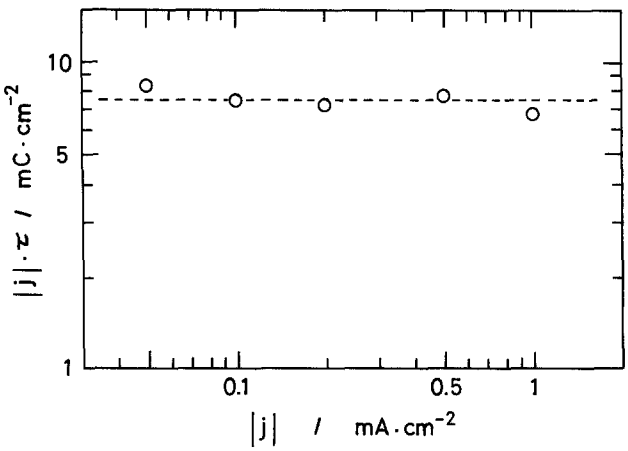


Fig. 4. The $|j| \cdot \tau$ vs. $|j|$ plots for the chronopotentiograms of the reduction of thin film of PB on Pt electrode in 1M KCl solution.

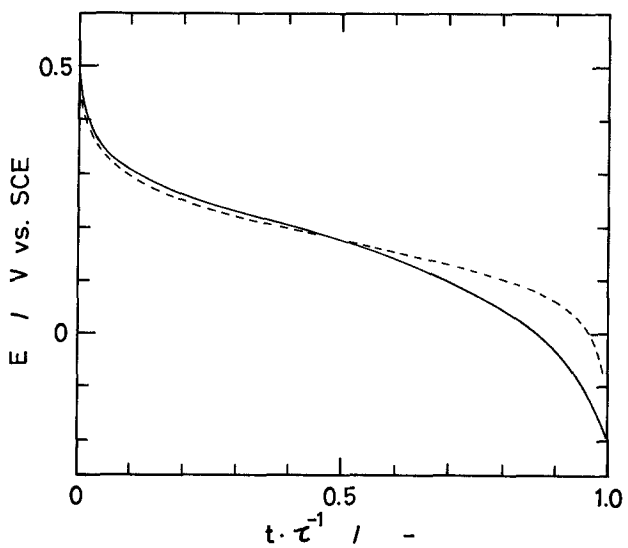


Fig. 5. Comparison between an observed chronopotentiogram (solid curve) for a thin film of PB in 1M KCl solution at 50 $\mu$A-cm$^{-2}$ and the calculated chronopotentiogram (dotted curve) from Eq. [9] with $n = 0.5$, $E_0 = +0.175$V vs. SCE, and $\tau = 169$s (experimentally obtained value).

*Optical absorption spectra.*—Figure 6 shows the optical absorption spectra of PB, ES, and BG on $In_2O_3$-coated glass electrode. The spectra of PB, ES, and BG were obtained at +0.5, −0.2, and +1.1V *vs.* SCE, respectively. The spectra observed agreed well with those of previous workers (18, 19).

In determining $X(E)$ from optical absorbance $A(E)$ from Eq. [10], absorbance at 720 nm was measured potentiostatically point by point in the potential range between +0.5 and −0.2V *vs.* SCE. $A_{max}$ and $A_{min.}$ were determined as the absorbance at +0.5 and −0.2V *vs.* SCE, respectively. Figure 7 shows the $E$ *vs.* $X(E)$ plots obtained from optical absorbances using Eq. [10] and [12]. The dotted curve in Fig. 7 shows the calculated curve from Eq. [12] with $E'_0 = +0.175$V *vs.* SCE and $n = 0.5$. The *in situ* optical data indicate that the observed electrode potential is thermodynamic potential.

From these voltammetric, chronopotentiometric, and spectroelectrochemical data, the equilibrium potential of PB/ES system is represented as the empirical formula

$$E = E_0 - \frac{2RT}{\mathbf{F}} \ln \frac{[Fe^{2+}]}{[Fe^{3+}]} + \frac{RT}{\mathbf{F}} \ln(a_{K^+}) \qquad [13]$$

where $[Fe^{2+}]$ and $[Fe^{3+}]$ denote the concentrations of $Fe^{2+}$ and $Fe^{3+}$, respectively, existing in the same ligand field in a solid matrix, and $a_{K^+}$ is the activity of $K^+$ ion in a solution.

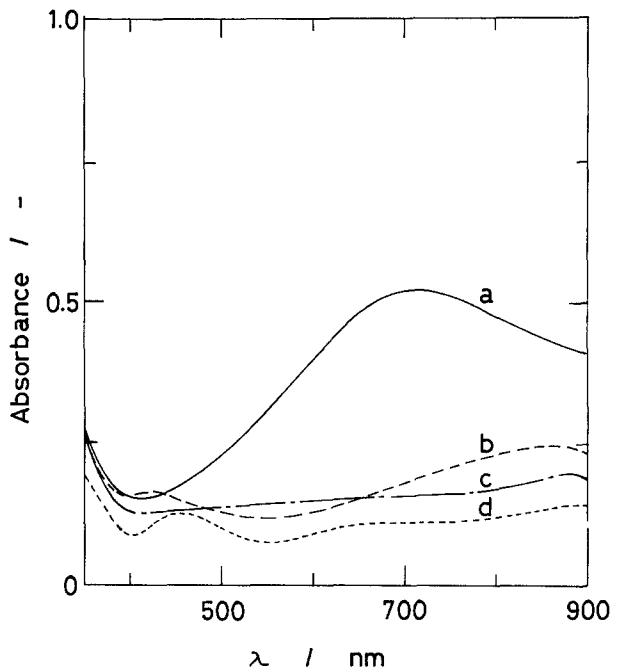


Fig. 6. Absorption spectra in the visible region for PB at +0.5V (a), BG at +1.1V (b), ES at −0.2V *vs.* SCE (c), and $In_2O_3$-coated glass only (d). The spectra were measured in KCl solution.

## Discussion

*PB/ES homogeneous-phase reaction.*–Ellis *et al.* (18) proposed the following equation for the reduction of PB

$$PB + K^+ + e^- \rightleftarrows ES \qquad [14]$$

and they used the Nernst equation directly to Eq. [14] in the form

$$E = E^\circ_0 + \frac{RT}{\mathbf{F}} \ln \left( \frac{a(PB)a(K^+)}{a(ES)} \right) \qquad [15]$$

where $a$(PB) and $a$(ES) were the activities of PB and ES, respectively, $a(K^+)$ is the activity of potassium ion in a solution, and $E^\circ_0$ is the standard electrode potential in Eq. [14]. In order to explain their results, they applied the theory of strictly regular solution on estimating $a$(PB) and $a$(ES) in Eq. [15], and they discussed the validity of the treatments based on Eq. [14] and [15].

The forms of Eq. [14] and the following Eq. [15] are the same as those applied by Johnson and Vosburgh (1) and Newmann and Roda (2) for the $MnO_2$/MnOOH system,

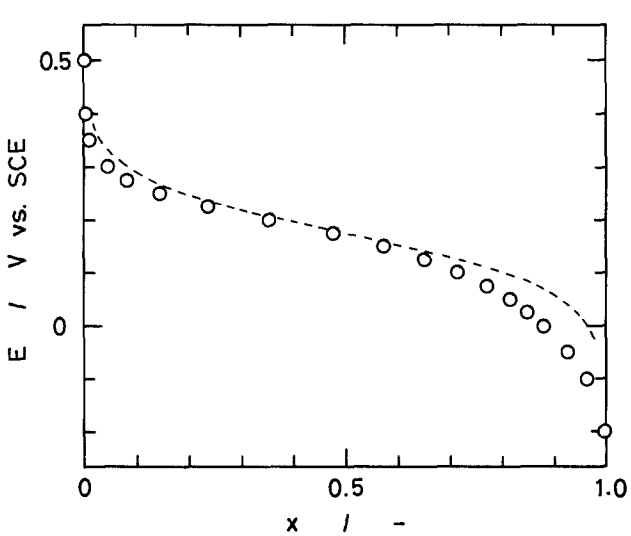


Fig. 7. The $E$ *vs.* $X$ plots obtained from the absorbance at 720 nm using Eq. [10] and [12]. Absorbance was measured potentiostatically point by point. The dotted curve was calculated from Eq. [12] with $E_0 = +0.175$V *vs.* SCE and $n = 0.5$.

and, consequently, $\alpha$(PB) and $\alpha$(ES) may be calculated by the Newmann and Roda's method (2). The specific definitions of PB (starting material) and ES (reduction product), however, seem to be difficult because the difference between PB and ES is the concentrations of $Fe^{2+}$ and $Fe^{3+}$ existing in the same ligand field and $K^+$ concentration in a solid matrix. In other words, PB is continuously converted to ES, isostructural with PB, by increasing $Fe^{2+}$ and $K^+$ concentration in a solid matrix during the reduction process.

Specific differences between the $Fe^{3+}/Fe^{2+}$ redox reaction in a solid matrix and in a solution are summarized in Table I. The differences between them are (*i*) the potential dependence with respect to $\ln([Fe^{2+}]/[Fe^{3+}])$ and (*ii*) the potential response of potassium ion, indicating that the redox reaction in a solid matrix is not explained by the analogy of the homogeneous redox reaction in a solution.

In recent years, Atlung and Jacobsen (9) have proposed a statistical mechanical treatment on dealing with an insertion electrode. We applied their basic concept to the analysis of PB/ES homogeneous-phase reaction. Instead of thinking about an electrode potential based on the Nernst equation using a chemical formula, the phase scheme (7, 8) of PB/ES electrode system in contact with an inert metal and electrolyte was considered, as is illustrated in Fig. 8a, in which $R^+$ transfer reaction is active.

PB has an electronic conduction which is assumed to proceed by a hopping mechanism, and it has an open structure to accommodate large metal cations and water molecules (15). The equilibrium of electrons at the phase boundary metal/PB, *i.e.*, $e^-$(metal) $\rightleftarrows$ $e^-$ (PB), shall be established. Also, the equilibrium of monovalent ion $R^+$ at the phase boundary PB/electrolyte, *i.e.*, $R^+$(PB) $\rightleftarrows$ $R^+$ (electrolyte), shall be established in such a system.

By applying Guggenheim's assumption to an electrochemical potential (29), one may write the equilibrium conditions in terms of electrochemical potentials for each species between phases

$$\bar{\mu}_e^{metal} = \bar{\mu}_e^{PB} \quad [16]$$

$$\bar{\mu}_R^{PB} \simeq \bar{\mu}_R^{E1} \quad [17]$$

where

$$\bar{\mu}_e^{PB} = \mu_e^{PB} - \mathbf{F}\phi^{PB} \quad [18]$$

$$\bar{\mu}_R^{PB} = \mu_R^{PB} + \mathbf{F}\phi^{PB} \quad [19]$$

$$\bar{\mu}_R^{E1} = \mu_R^{E1} + \mathbf{F}\phi^{E1} \quad [20]$$

By arranging the equations and converting the potential scale, one may have the following expression for the

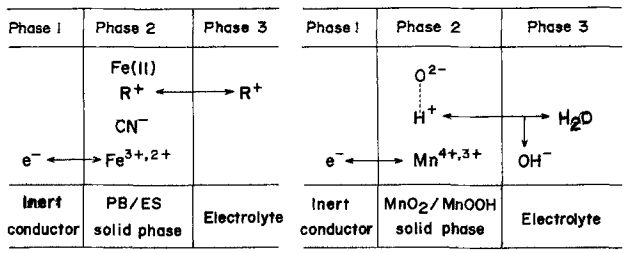


**Fig. 8. Phase scheme a: PB/ES homogeneous-phase system in contact with an inert conductor and electrolyte. $R^+$ (monovalent ion) transfer reaction is active. Fe(II) is inactive for PB/ES reaction. b: $MnO_2$/MnOOH homogeneous-phase system in contact with an inert conductor and electrolyte. Proton transfer reaction is active.**

electrode potential

$$E = \frac{\mu_R^{E1}}{\mathbf{F}} - \frac{(\mu_e^{PB} + \mu_R^{PB})}{\mathbf{F}} \quad [21]$$

in which $\mu_R^{E1}$ denotes the chemical potential of $R^+$ ion in an electrolyte, and $\mu_e^{PB}$ and $\mu_R^{PB}$ denote the chemical potentials of electron and $R^+$ ion, respectively, in a PB solid matrix. The chemical potential of $R^+$ ion in an electrolyte, $\mu_R^{E1}$, can be represented in terms of the standard chemical potential, $\mu_R^{\phi E1}$, and the activity of $R^+$ ion in an electrolyte, $a_R$, as

$$\mu_R^{E1} = \mu_R^{\phi E1} + RT \ln (a_R) \quad [22]$$

On the other hand, $\mu_e^{PB}$ and $\mu_R^{PB}$ are defined as

$$\frac{\mu_e^{PB}}{N_0} = \left(\frac{\partial G}{\partial n_e}\right) \quad \frac{\mu_R^{PB}}{N_0} = \left(\frac{\partial G}{\partial n_R}\right) \quad [23]$$

where $N_0$ is Avogadro's number.

When PB is reduced electrochemically, $Fe^{3+}$ existing in a certain ligand field in a matrix is reduced to $Fe^{2+}$ in the same ligand field and $R^+$ ion is inserted into a matrix in order to compensate the additional charge. Electrons and $R^+$ ions seem to move independently through different sites in the matrix. In such a case, one may formulate $\mu_e^{PB}$ and $\mu_R^{PB}$ as

$$\frac{\mu_e^{PB}}{N_0} = \left(\frac{\partial G}{\partial n_e}\right) \simeq \left(\frac{\partial \mathbf{F}}{\partial n_e}\right) = -kT\left(\frac{\partial \ln Z_e}{\partial n_e}\right) \quad [24]$$

and

$$\frac{\mu_R^{PB}}{N_0} = \left(\frac{\partial G}{\partial n_R}\right) \simeq \left(\frac{\partial \mathbf{F}}{\partial n_R}\right) = -kT\left(\frac{\partial \ln Z_R}{\partial n_R}\right) \quad [25]$$

**Table I. Specific differences between the electrochemical behavior of Prussian blue/Everitt's salt redox reaction and $Fe(CN)_6^{3-}/Fe(CN)_6^{4-}$ redox reaction in a solution**

| Redox reaction | $Fe(CN)_6^{3-}/Fe(CN)_6^{4-}$ | Prussian blue/Everitt's salt |
|---|---|---|
| System | Redox reaction of soluble species | Redox reaction in thin film of solid |
| Voltammetry | | |
| Shape | Not symmetrical about peak position[a] | Symmetrical about peak position |
| Midpoint of anodic and cathodic peak[b] | +210 mV *vs.* SCE | +200 mV *vs.* SCE |
| pH response | Yes[c] | No |
| pK response | No | Yes |
| Chronopotentiometry[d] | | |
| $E_0$ | +215 mV *vs.* SCE | +175 mV *vs.* SCE |
| $n$ | 1.0 | 0.5 |

[a] If thin liquid film was used, voltammetric peaks symmetrical about the peak position would be obtained.
[b] Measured in 1*M* KCl solution.
[c] Due to the protonation of $Fe(CN)_6^{4-}$.
[d] $E_0$ and $n$ were determined from the equation

$$E = E_0 + \frac{RT}{n\mathbf{F}} \ln \frac{1 - (t/\tau)^{1/2}}{(t/\tau)^{1/2}}$$

for the reduction of 0.02M $Fe(CN)_6^{3-}$ in 1*M* KCl, and from Eq. [6] for the reduction of PB.

where $Z_e$ and $Z_R$ are the partition functions with respect to electrons and $R^+$ ions, respectively, and $p\,\Delta\,V \simeq 0$ is assumed. Combination of Eq. [21], [22], [24], and [25] gives a general expression on the electrode potential for the reaction, if the partition function $Z_e$ and $Z_R$ are known from electronic structure, crystal structure, interaction between charged species, and so forth.

If the work to put electrons into $Fe^{3+}$ in a matrix is the same for all subsequent steps, which corresponds to a redox reaction between the well-defined oxidation states of ions, the partition function of electrons for such a case would be represented as (30, 31)

$$Z_e\,(T, V, n_e) \simeq \frac{n_0{}^e!}{n_e!(n_0{}^e - n_e)!} \exp\left(-\frac{n_e\epsilon_0}{kT}\right) \qquad [26]$$

where $n_0{}^e$, $n_e$, and $(n_0{}^e - n_e)$ are the number of available sites, the number of occupied sites ($Fe^{2+}$ in this case), and the number of unoccupied sites ($Fe^{3+}$ in this case), respectively, while $\epsilon_0$ is an energy.

Putting Eq. [26] into Eq. [24], one may have the following expression after applying the Stirling's approximation

$$\mu_e{}^{PB} = \mu_e{}^{\phi PB} + RT \ln \frac{n_e}{(n_0{}^e - n_e)} \qquad [27]$$

where $\mu_e{}^{\phi PB}$ is the standard chemical potential of electron in PB/ES system.

The same treatment could be made with respect to $R^+$ ion in a matix

$$\mu_R{}^{PB} = \mu_R{}^{\phi PB} + RT \ln \frac{n_R}{(n_0{}^R - n_R)} \qquad [28]$$

where $n_0{}^R$, $n_R$, and $(n_0{}^R - n_R)$ are the number of available sites, the number of occupied sites, and the number of unoccupied sites, respectively, with respect to $R^+$ ion in a matrix.

For PB/ES system, the number of available sites for electrons and $R^+$ ions would be the same (21), *i.e.*, $n_0{}^e = n_0{}^R = n_0$, and then the combination of Eq. [21], [22], [27], and [28] gives

$$E = E_0 + \frac{RT}{\mathbf{F}} \ln(a_R) - \frac{RT}{\mathbf{F}} \ln \frac{n_e}{(n_0 - n_e)} - \frac{RT}{\mathbf{F}} \ln \frac{n_R}{(n_0 - n_R)} \qquad [29]$$

where

$$E_0 = \frac{\mu_R{}^{\phi E1}}{\mathbf{F}} - \frac{(\mu_e{}^{\phi PB} + \mu_R{}^{\phi PB})}{\mathbf{F}} \qquad [30]$$

According to Eq. [29], the 59 mV dependence at 25°C with respect to log ($a_R$) and −59 mV potential dependences in terms of log $(n_e/[n_0 - n_e])$ and log $(n_R/[n_0 - n_R])$ would be expected, and then the standard electrode potential of PB/ES system, $E_0$, would be obtained putting $a_R = 1$, $n_e = n_0/2$, and $n_R = n_0/2$.

The condition of electroneutrality requires $n_e = n_R$, then Eq. [29] becomes

$$E = E_0 - \frac{2RT}{\mathbf{H}} \ln \frac{X}{(1 - X)} + \frac{RT}{\mathbf{F}} \ln (a_R) \qquad [31]$$

or

$$E = E_0 - \frac{2RT}{\mathbf{F}} \ln \frac{[Fe^{2+}]}{[Fe^{3+}]} + \frac{RT}{\mathbf{F}} \ln (a_R)$$

where $X = n_e/n_0$, *i.e.*, the mole fraction of $Fe^{2+}$.

Equation [31] is the same as the empirical formula [13]. Thus, we have concluded that the observed potential dependence $-2RT/\mathbf{F}$ with respect to ln $([Fe^{2+}]/[Fe^{3+}])$ can be derived from the effect of $R^+$ ion ($K^+$ ion, in the present case) in a solid matrix on the electrode potential. In other words, the effect is associated with entropy due to the distribution of $R^+$ ion in a solid matrix.

*$MnO_2$/MnOOH homogeneous-phase reaction ($Mn^{4+}/Mn^{3+}$ redox reaction in a solid matrix).*—Bode *et al.* (32) first studied the chemical reduction of $MnO_2$S, and they found the reduction in homogeneous phase is typical of gamma-$MnO_2$ down to $MnO_{1.5}$. Although the term "gamma" is not specific (33), there is a general agreement that both chemical and electrochemical reduction of gamma modification proceed in homogeneous phase (1-4, 10-13, 32, 34-36).

In recent years, Swinkels *et al.* (12) proposed that three or more overlapping discharge processes, each of which is of the simple one-electron type but with different $E_0$'s, must be considered for an explanation of the larger prelogarithmic factor in the Nernst equation, about twice the −59 mV expected for one-electron transfer. More recently, Ruetschi (38) reported the cation-vacancy model for $MnO_2$ and formulated the electrode potential of $MnO_2$ based on his model. We, however, prefer to extend the homogeneous phase theory (3, 4) from the analogy of the PB/ES system.

A schematic phase scheme for the $MnO_2$/MnOOH homogeneous phase is given in Fig. 8b. For the reduction of $MnO_2$, $Mn^{4+}$ is reduced to $Mn^{3+}$ in a homogeneous solid phase by the arrival of electron together with the formation of new hydroxyl group with proton from a solution, which was confirmed by XRD and IR studies on $MnO_2$/MnOOH systems (37). In this case, proton transfer at the interface is active.

By comparing the two homogeneous-phase reactions, we may discuss the electrode potential of $MnO_2$/MnOOH homogeneous phase. In the reduction process of PB, electrons and $R^+$ ions are introduced into the matrix of PB. The concentrations of $Fe^{2+}$ ions and $R^+$ ions in the lattice increase gradually, and, finally, PB is converted to ES, isostructural with PB. In such a case, we can formulate the electrode potential of PB/ES homogeneous phase as Eq. [31], in which the potential dependence with respect to log $([Fe^{2+}]/[Fe^{3+}])$ appeared as $-2.303 \times 2RT/\mathbf{F}$ (*i.e.*, −118 mV at 25°C) due to the effect of $R^+$ ion in a solid matrix as was discussed in the previous section.

It should be recalled here that there are two types of iron sites in PB matrix. One is carbon-coordinated iron (low spin), and the other is nitrogen-coordinated iron (high spin). Because of this, the $Fe^{3+}/Fe^{2+}$ redox reaction in the solid matrix takes at two different electrode potentials, *i.e.*, PB/ES reaction at *ca.* +0.2V *vs.* SCE and PB/BG at *ca.* +0.9V in 1*M* KCl solution. Thus, the redox potentials appear with a large voltage separation due to the effect of ligand field. For the $MnO_2$/MnOOH homogeneous system, such a voltage separation may not occur because all manganese ions exist in the same ligand field (oxygen-coordinated manganese). During the reduction of $MnO_2$, the concentrations of $Mn^{3+}$ ions and $OH^-$ ions in a solid matrix increase gradually, and, finally, $MnO_2$ is converted to MnOOH, isostructural with original $MnO_2$ (37). In the $MnO_2$/MnOOH homogeneous phase, electrons move freely along $Mn^{4+,3+}$ sites in the lattice and also proton jump one $O^{2-}$ site to another. Such a situation is very similar to that of PB/ES system. Thus, the previous treatments for the PB/ES system can be made for the $MnO_2$/MnOOH system.

Kozawa and Powers (3, 4) formulated the electrode potential of $MnO_2$/MnOOH homogeneous phase as Eq. [3] from the analogy of a redox reaction in a solution. They referred to $Fe^{3+}/Fe^{2+}$ redox reaction in an acid solution as a model for $MnO_2$/MnOOH homogeneous-phase reaction in order to interpret their homogeneous phase theory. The electrochemical character of $Fe^{3+}/Fe^{2+}$ redox reaction in homogeneous solution phase, however, is different from that in homogeneous solid phase as examined here.

The specific effect of solution *p*H on the potential response would be due to the proton transfer in the $MnO_2$/MnOOH homogeneous solid phase, which may be deduced from Vetter's general theories (7, 8). The inserted protons also affect the electrode potential because of the formation of hydroxyl group (enthalpy factor) and their distribution in a solid matrix (entropy factor) in addition to $Mn^{4+}/Mn^{3+}$ redox reaction. The above description would be the core meaning of proton-electron mechanism (3, 4).

It is therefore reasonable to deduce that the electrode potential of the $MnO_2$/MnOOH homogeneous-phase sys-

tem is expressed as

$$E = E_0 - \frac{2RT}{F} \ln \frac{[Mn^{3+}]}{[Mn^{4+}]} + \frac{RT}{F} \ln (a_{H^+}) \qquad [32]$$

by taking into account for the effect of proton ($OH^-$ ion, in fact) in a solid matrix on the electrode potential. Then, if the electrode potentials of $MnO_2$/MnOOH system were measured as a function of log ($[Mn^{3+}]/[Mn^{4+}]$) at constant pH and if the conditions were well fit to the conditions required by the previous treatments, −118 mV of potential dependence would be observed in this case. Some deviations from Eq. [32], however, may be observed in experimental curves, especially in latter half of the discharge curves, partly because of the secondary modification of discharge product and partly because of the change of ligand field around manganese ion due to the coordination of $OH^-$ ion, which is not the case for the PB/ES system. Tye (10, 13) suggested that the discharge of $MnO_2$ involved two regions (one between $MnO_{2.0}$ and $MnO_{1.75}$ and the other between $MnO_{1.75}$ and $MnO_{1.5}$), assuming the intermediate compound $MnO_{1.75}$, like a PB (50% $Fe^{2+}$, 50% $Fe^{3+}$ material) between ES (100% $Fe^{2+}$ material) and BG (100% $Fe^{3+}$ material). This may be true, but the specific intermediate compound of $MnO_{1.75}$ has not been observed yet (37).

A possible refinement of Eq. [32] as to how the partition function in Eq. [26] can be modified in considering the additional factors, especially the change of ligand field around manganese ion due to the coordination of $OH^-$ ion combined with crystal structure and the electronic structure of the $MnO_2$/MnOOH system, will be discussed in future papers together with the experimental and analytical results of $MnO_2$.

## Acknowledgment

The present work was partially supported by a grant in aid for Scientific Research from the Ministry of Education, Science and Culture.

Manuscript submitted April 6, 1985; revised manuscript received Aug. 15, 1985.

*Okayama University assisted in meeting the publication costs of this article.*

## REFERENCES

1. R. S. Johnson and W. C. Vosburgh, *This Journal*, **100,** 471 (1953).
2. K. Newmann and E. Roda, *Ber. Bunsenges. Phys. Chem.*, **69,** 347 (1965).
3. A. Kozawa and R. A. Powers, *This Journal*, **113,** 870 (1966).
4. A. Kozawa and R. A. Powers, *Electrochem. Technol.*, **5,** 533 (1967).
5. F. L. Tye, *Electrochim. Acta.*, **21,** 415 (1976).
6. T. Ohzuku, C. Ishibashi, and T. Hirai, Extended Abstracts of The 33rd Battery Symposium in Japan, Yokohama, p. 87, Nov. 1982.
7. K. J. Vetter, *This Journal*, **110,** 597 (1963).
8. K. J. Vetter and N. Jaeger, *Electrochim. Acta*, **11,** 401 (1966).
9. S. Atlung and T. Jacobsen, *ibid.*, **26,** 1447 (1981).
10. W. C. Maskell, J. E. A. Shaw, and F. L. Tye, *ibid.*, **28,** 225 (1983).
11. W. C. Maskell, J. E. A. Shaw, and F. L. Tye, *ibid.*, **28,** 231 (1983).
12. D. A. J. Swinkels, K. E. Anthony, P. M. Fredericks, and P. R. Osborn, *J. Electroanal. Chem.*, **168,** 433 (1984).
13. F. L. Tye, *Electrochim. Acta*, **30,** 17 (1985).
14. D. F. Shriver, *Struct. Bonding (Berlin)*, **1,** 32 (1966).
15. M. B. Robin and P. Day, *Adv. Inorg. Chem. Radiochem.*, **10,** 247 (1967).
16. L. Ludi and U. Güdel, *Struct. Bonding (Berlin)*, **14,** 1 (1973).
17. V. D. Neff, *This Journal*, **125,** 886 (1978).
18. D. Ellis, M. Eckhoff, and V. D. Neff, *J. Phys. Chem.*, **85,** 1225 (1981).
19. K. Itaya, H. Akahoski, and S. Toshima, *This Journal*, **129,** 1498 (1982).
20. K. Itaya, T. Ataka, and S. Toshima, *J. Am. Chem. Soc.*, **104,** 4767 (1982).
21. J. F. Keggin and F. D. Miles, *Nature*, **137,** 577 (1936).
22. F. Herren, P. Fischer, A. Ludi, and W. Hälg, *Inorg. Chem.*, **19,** 956 (1980).
23. L. M. Epstein, *J. Chem. Phys.*, **36,** 2731 (1962).
24. J. F. Duncan and P. W. R. Wigley, *J. Chem. Soc.*, 1120 (1963).
25. D. Davidson and L. A. Welo, *J. Phys. Chem.*, **32,** 1191 (1928).
26. G. Emschwiller, *C. R. Acad. Sci.*, **238,** 1414 (1954).
27. H. B. Weiser, W. O. Milligan, and J. B. Bates, *J. Phys. Chem.*, **46,** 99 (1942).
28. A. T. Hubbard and F. C. Anson, *Anal. Chem.*, **38,** 58 (1966).
29. E. A. Guggenheim, *J. Phys. Chem.*, **33,** 842 (1929).
30. R. Kubo, "Netsugaku-Tokeirikigaku (Thermodynamics and Statistical Mechanics)," Shokabo Co. Ltd., Tokyo (1961).
31. R. Kubo, "Tokeirikigaku (Statistical Thermodynamics)," Kyoritsu Shuppan Co. Ltd., Tokyo (1971).
32. H. Bode, A. Schmier, and D. Berndt, *Z. Elektrochem.*, **66,** 586 (1962).
33. T. Ohzuku, H. Higashimura, and T. Hirai, *Electrochim. Acta*, **29,** 779 (1984).
34. J. P. Gavano, B. Morignat, E. Fialdes, B. Emery, and J. F. Laurent, *Z. Phys. Chem.*, **46,** 359 (1965).
35. R. Giovanoli and U. Leuenberger, *Helv. Chim. Acta*, **52,** 2333 (1969).
36. W. C. Maskell, J. E. A. Shaw, and F. L. Tye, *Electrochim. Acta*, **26,** 1403 (1981).
37. T. Ohzuku and T. Hirai, in "Manganese Dioxide Electrode Theory and Practice for Electrochemical Applications," B. Schumm, Jr., R. L. Middaugh, M. P. Grotheer, and J. C. Hunter, Editors p. 141, The Electrochemical Society Softbound Proceedings Series, Pennington, NJ (1984).
38. P. Ruetschi, *This Journal*, **131,** 2737 (1984).